

Πρακτικά		4ου Συνεδρίου		Μάιος 1988	
Δελτ. Ελλην. Γεωλ. Εταιρ.	Τομ. XXIII/3	σελ. 157-172	Αθήνα 1989		
Bull. Geol. Soc. Greece	Vol.	pag.	Athens		

3-DIMENSIONAL VELOCITY STRUCTURE OF NORTH-CENTRAL GREECE FROM INVERSION OF TRAVEL TIMES

G. DRAKATOS, J. LATOUSSAKIS, G. STAVRAKAKIS, D. PAPANASTASSIOU, J. DRAKOPOULOS *

ABSTRACT

Three dimensional velocity structure of the upper crust is determined by inversion of P-waves in the region between 38.7°N - 41.2°N and 22.3°E - 24.4°E.

46 events and 16 stations, all of them located in the above mentioned region, are used. The data are inverted following the method of AKI and LEE.

For the upper 15 Km of the crust the results show a strong effect of the local surficial geology. Low velocities are predominant around Pagassitikos Gulf, North Euboea and Thermaikos Gulf, where geothermal area, fracture zones and sedimentary layers exist. High velocities are obtained in the northern part of the region, where geologically old and stable massives (Servomacedonian, Rhodope) are predominant.

ΕΥΝΟΨΗ

Προσδιορίζεται τρισδιάστατο μοντέλο ταχυτήτων στον ανώτερο φλοιό, με αντιστροφή των P κυμάτων, στην περιοχή μεταξύ των 38.7°N - 41.2°N και 22.3°E - 24.4°E.

Χρησιμοποιούνται για το σκοπό αυτό 46 σεισμοί και 16 σταθμοί που ευρίσκονται στην προαναφερθείσα περιοχή. Τα δεδομένα αντιστρέφονται με την μέθοδο των AKI και LEE.

Για τα πρώτα 15 Km του φλοιού, τα αποτελέσματα δείχνουν μια ισχυρή επίδραση των τοπικών γεωλογικών συνθηκών. Χαμηλές τιμές ταχυτήτων επικρατούν γύρω από τον Παγασητικό Κόλπο, την Βόρεια Εύβοια και τον Θερραϊκό Κόλπο, όπου αναντούν γεωθερμικά πεδία, ρηζιγενείς ζώνες και ιζήματα.

Υψηλές τιμές υπολογίσθησαν για τις ταχύτερες στο βόρειο τμήμα της περιοχής, όπου υπάρχουν παλαιοί γεωλογικοί σχηματισμοί (Μάζα της Ροδόπης, Σερβομακεδονική Ζώνη).

ΕΙΣΑΓΩΓΗ - INTRODUCTION

The last ten years, it is widely accepted that one of the most powerful methods to investigate three-dimensional velocity structure of the earth, is the inversion of residuals from arrival times data (AKI and LEE, 1976; AKI et al., 1977; ISHIDA, 1984; SPARKMAN, 1986) or the inversion of macroseismic intensities data (HASHIDA et al., 1987).

In the present paper, the method developed by AKI and LEE (1976) is used, an outline of which is described below. Residuals

Γ. ΔΡΑΚΑΤΟΣ, Ι. ΛΑΤΟΥΣΣΑΚΗΣ, Γ. ΣΤΑΥΡΑΚΑΚΗΣ, Δ. ΠΑΠΑΝΑΣΤΑΣΙΟΥ και
Ι. ΔΡΑΚΟΠΟΥΛΟΣ - ΤΡΙΣΔΙΑΣΤΑΤΟ ΜΟΝΤΕΛΟ ΤΑΧΥΤΗΤΩΝ ΣΤΗΝ ΒΟΡΕΙΟ ΚΑΙ
ΚΕΝΤΡΙΚΗ ΕΛΛΑΔΑ ΜΕ ΑΝΤΙΣΤΡΟΦΗ ΤΩΝ ΧΡΟΝΩΝ ΔΙΑΔΡΟΜΗΣ

* National Observatory of Athens, Department of Geology, Institute
P. O. Box 20048, GR 11810, Athens, Greece.

are caused due to the perturbation of initial source parameters and due to the slowness perturbation of seismic rays which penetrate the earth, travelling from hypocenter to the stations. This method estimates the percentage of each residual due to the above mentioned reasons.

Interesting geophysical and geological features in Central and Northern Greece (Fig. 1) and the existence of a dense (in comparison to other regions in Greece) network of 16 stations give rise to the investigation in this region, in an attempt to extract information about the three-dimensional velocity structure of the upper crust.

Residuals from arrival times of Pg and P* waves are used. Due to the lack of deep events only the velocity structure of upper crust is investigated.

ΤΕΚΤΟΝΙΚΟ ΣΑΘΕΤΩΣ - TECTONIC SETTING

The study region, where crustal extension occurred in the middle Miocene time, lies at the north of the Hellenic volcanic arc (Fig. 2).

Axios-Vardar zone, Servomacedonian and Rhodope massives are the predominant seismotectonic features in the northern part of the region (Fig. 1). Axios-Vardar zone is an elongated basin, striking NNW-SSE through Yugoslavia and Northern Greece. Rhodope massif is a geologically old (of Precambrian age) and seismologically stable region of low seismicity, comprised of metamorphic rocks. Servomacedonian massif of Paleozoic age, consists of metamorphic rocks too.

In the Central-Eastern part of the region, predominant features are the Sporades graben (DEWEY and SENGOR, 1979) and the extension of North Anatolian Fault (McKENZIE, 1972). It has been shown (PAPAZACHOS et al., 1979(a)) that the highest seismic activity in Northern Greece and the surrounding area, during the present century, has occurred along Servomacedonian massif, which extends to the East along the northernmost part of the Aegean area and joins the North Anatolian seismic zone (COMNINAKIS and PAPAZACHOS, 1981).

The thickness of the crust is about 30 Km, according to deep seismic soundings (MAKRIS, 1978(b)).

The thickness of the sedimentary layer in North Aegean Sea is about 3 Km (MAKRIS, 1978(a)). Two drill holes in Thermaikos Gulf, penetrated 3.5 Km of sediments (FAUGERES and ROBERT, 1976).

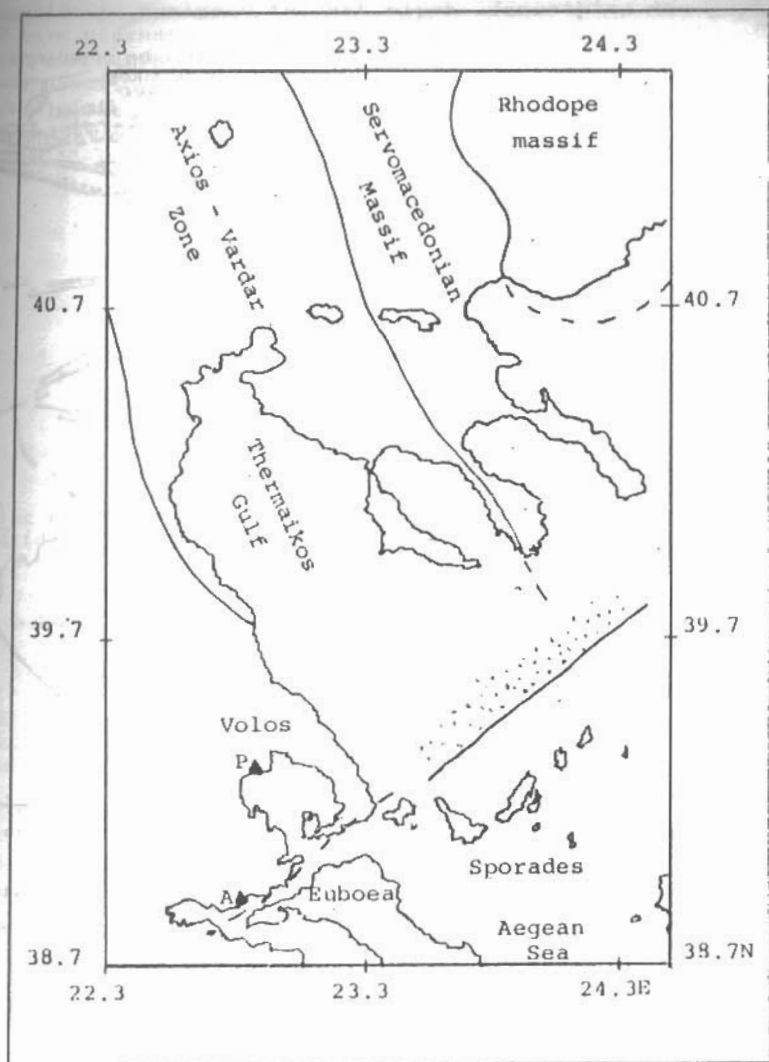
Positive Bouguer anomalies with a maximum about 150 mgl characterize the region (MAKRIS, 1975).

In the Southwestern part of the region, fracture zones (DEWEY and SENGOR, 1979) and volcanoes (Fig. 1) of the westernmost part of the Hellenic volcanic arc (NINKOVITCH and HAYS, 1972; FYTIKAS et al., 1976) are predominant.

The investigating region is a back arc basin. The most of earthquakes are shallow and tension axes T generally strikes N-S because of the coverage of African and Aegean plates, as it was proved by focal mechanism studies (McKENZIE, 1978; PAPAZACHOS and COMNINAKIS, 1978; DRAKOPOULOS and DELIBASIS, 1983).

ΜΕΘΟΔΟΛΟΓΙΑ - METHOD

In the present study, the method of AKI and LEE has been used. The earth's structure is modeled in rectangular blocks and



STUDY REGION

Scale 1:2500000

Fig. 1 Simplified summary of Northwest Aegean tectonics, following COMNINAKIS and PAPAZACHOS (1981), DEWEY and SENGÖR (1979). The heavy line and the broken line are a fault and a poorly defined fault, respectively. The stippled area shows a Neogene Quaternary graben. Solid triangles are volcanoes (NINKOVITCH and HAYS 1972; FYTIKAS et al., 1976) P: Porphyriou and A: Achilleion.

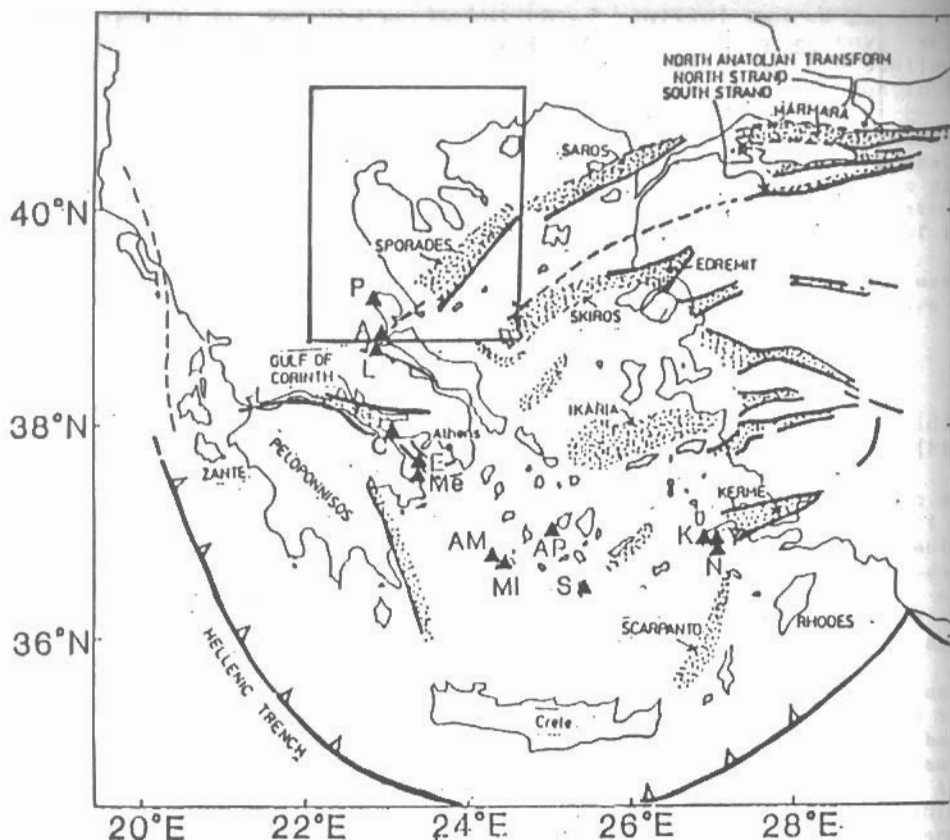


Fig. 2 Simplified summary of Greek tectonics. For explanation of symbols see caption of Fig. 1. The study region is indicated in the frame.

TABLE 1. Coordinates and corrections of stations

Code	Lat (N)	Lon (E)	Hgh (m)	C (sec)
PIG	40.37	23.44	580	10.10
SOH	40.82	23.35	670	10.11
LIT	40.10	22.49	400	10.08
GRG	40.95	22.40	560	10.09
PAIG	39.93	23.68	140	10.02
KNT	41.16	22.90	380	10.06
OUR	40.33	23.98	60	10.01
SRS	41.12	23.59	400	10.07
THE	40.63	22.96	70	10.01
VSI	38.88	23.21	448	10.07
VGI	39.44	22.88	424	10.07
VFI	39.23	22.59	360	10.06
VNE	39.31	23.23	692	10.12
VSK	39.11	23.69	374	10.06
VPA	38.78	22.34	1084	10.18
VMA	38.71	23.59	460	10.08

a parameter is assigned to each block, describing the perturbation of P wave slowness in the block. The data set consists of first P arrival times of M earthquakes, observed at N stations.

By denoting the P arrival time from the j^{th} earthquake, observed at the i^{th} station as T_{ij}^{obs} , the arrival time is given by

$$T_{ij}^{obs} = T_{ij}^{calc} + (dT/dX)_{ij} DX_j + (dT/dY)_{ij} DY_j + (dT/dZ)_{ij} DZ_j + DT_j + \sum_k (ET_{ij}^{(k)} F_k) + E_{ij} \quad (1)$$

where,

T_{ij}^{calc} : the calculated P arrival time,
 $(dT/dX)_{ij}, (dT/dY)_{ij}, (dT/dZ)_{ij}$: derivatives of travel times with respect to X, Y and Z coordinates of the hypocenter, respectively,
 DT_j, DX_j, DY_j, DZ_j : corrections to the source parameters of the j^{th} event,
 $ET_{ij}^{(k)} F_k$: travel time variation due to the slowness perturbation in block k,
 F_k : slowness perturbation in block k and
 E_{ij} : higher order terms and errors in observation

Writing observed minus calculated time (O-C) as a vector \bar{d}

$$\bar{d} = (d_{11}, d_{21}, \dots, d_{m1}, d_{12}, \dots, d_{m2}, \dots, d_{mM}) \quad (2)$$

where, \bar{d} denotes the transpose of d , equation (1) is transformed to

$$\bar{d} = A\bar{m} + \bar{e} \quad (3)$$

where,

A is a $NM \times (4M+K)$ matrix with components given in (1)
 \bar{m} is a transpose of vector m , with components $(DX_1, DY_1, DZ_1, DT_1, \dots, DX_M, \dots, DT_M, F_1, \dots, F_k)$
 \bar{e} is the error vector with components E_{ij} .

In order to avoid an unstable solution, which satisfies the equation

$$\bar{\lambda} \bar{\lambda} \bar{m} = \bar{\lambda} \bar{d} \quad (4)$$

a damped least squares method is used:

$$(\bar{\lambda} \bar{\lambda} + O) \bar{m} = \bar{\lambda} \bar{d} \quad (5)$$

where, O is a diagonal matrix with positive elements δ_i , according to LEVENBERG (1944).

Then the damped least squares solution is given as

$$\bar{m} = (\bar{\lambda} \bar{\lambda} + O)^{-1} \bar{\lambda} \bar{d} \quad (6)$$

where,

\bar{m} is the solution which minimizes the

$|\bar{m} - \bar{d}|^2$ and $|\bar{m}|^2$, simultaneously.

Therefore, the resolution matrix in this case is given by

$$R = (\bar{\lambda} \bar{\lambda} + O)^{-1} \bar{\lambda} \bar{\lambda} \quad (7)$$

As it has been shown by WIGGINS (1972), the magnitude of diagonal element is a measure of the resolution. If R is the identity

matrix, the solution is completely resolved.
The covariance matrix D , is given by

$$D = \sigma_d^2 R(\bar{A}A + O)^{-1} \quad (8)$$

where, σ_d^2 is the variance of errors in the data.

ΑΝΑΛΥΣΗ ΛΕΓΟΜΕΝΩΝ ΚΑΙ ΔΙΑΔΙΚΑΣΙΑ ΑΝΤΙΕΠΙΣΤΡΟΦΗΣ DATA ANALYSIS AND INVERSION PROCEDURE

The data used in this study are arrival times of P_g - and P^* waves at 16 stations (Table 1), in the area included between $38.7^\circ N - 41.2^\circ N$ and $22.3^\circ E - 24.4^\circ E$ (Fig. 1)

The Geophysical Department of the Aristotelian University of Thessaloniki has installed a network of 8 seismological stations, in the area under investigation since 1982. An other temporary network of 9 stations has been installed in the study region and the surrounding area from the Geophysical Department of Athens University, since 1983. This network operated up to 1985. Only 7 stations of the above mentioned network are used. Furthermore, one more station of the "National Seismological Network" has been incorporated in the analysis.

Many earthquakes were recorded since the operation of the stations and finally 46 earthquakes, of which the hypocenters are located in the investigating region, are selected (Table 2). Main criterion for their choice is their spatial distribution, in order to obtain a stable and reliable solution. A second criterion is the number of stations to which each event has been recorded, in order to obtain a large number of arrival times (data). The selected events are independent than magnitude and their focal depths lie between 1 Km to 23 Km. The arrival times and the parameters of each event, are those published in ISC bulletin

The earth's crust beneath the investigated region is divided into two horizontal layers, of 15 Km thickness. Each layer is divided into 6×10 rectangular blocks in E-W and N-S directions, respectively. Flat layer structure is assumed because of the small area of the region. The block sizes in E-W and N-S directions, are 31 Km and 30 Km, respectively. The block configurations, the events and the stations used, are shown in Fig. 3.

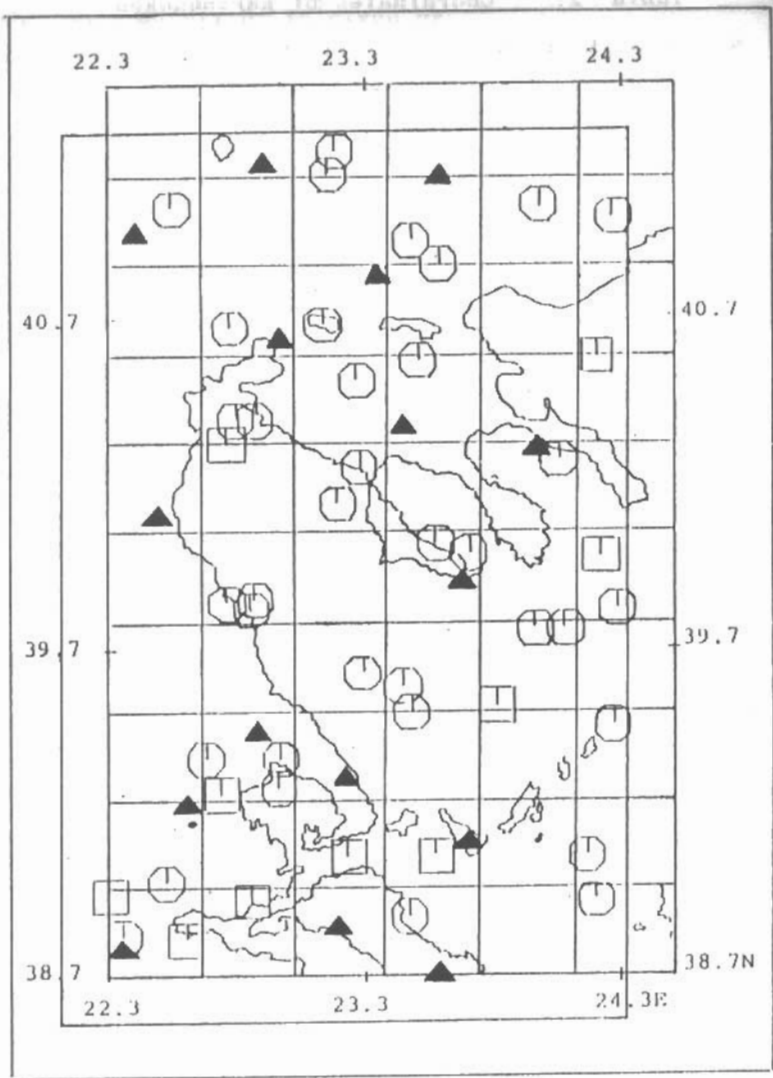
In total, 346 residuals data are inverted. The number of unknown parameters, given theoretically as $4 \times M \times K$, is 304. Actually, only 55 blocks in the upper layer and 32 in the lower one are penetrated by seismic rays. Therefore, the effective number of unknown parameters is reduced to 271.

When the data are from local earthquakes, the source parameters such as origin time and location of earthquakes, must be considered as unknown parameters (HORIE and AKI, 1982). It has been shown (PAVLIS and BOOKER, 1980; SPENCER and GUBBINS, 1980) that the source parameters can be eliminated from the equations and the problem may involve only the structure parameters, especially when a large number of earthquakes is dealt with.

Since, the inversion procedure is time consuming, the number of earthquakes is restricted to 46. Therefore, a direct elimination of hypocenter parameters is not adequate. However, by using these seismic events, a sufficient distribution is obtained. The hypocenters are relocated before the inversion procedure and to minimize the effect of events parameters, high values are assigned to the square roots of damping factors. For the X, Y and Z

Table 2. Coordinates of Earthquakes

N	Year	M	D	h:m:s	lat(N)	lon(E)	Dpt(Km)
1	1982	07	08	022145.6	41.00	24.27	10
2	1982	08	07	174610.8	40.57	23.51	10
3	1982	10	09	075109.8	41.13	23.16	13
4	1983	01	01	060419.8	39.26	22.73	20
5	1983	01	09	185427.8	40.68	23.14	5
6	1983	01	19	152547.4	39.53	23.81	23
7	1983	01	19	171100.3	39.07	23.58	17
8	1983	01	20	050159.6	38.81	22.59	20
9	1983	01	21	061507.0	39.28	22.96	2
10	1983	01	29	101116.2	40.51	23.27	9
11	1983	02	27	032607.7	38.95	22.30	21
12	1983	02	27	035221.9	39.59	23.45	4
13	1983	03	19	094851.6	39.07	23.23	17
14	1983	03	29	153925.5	38.88	23.47	12
15	1983	04	03	064107.5	40.67	22.77	10
16	1983	04	05	063600.9	39.76	23.96	13
17	1983	04	05	081441.5	39.37	22.67	4
18	1983	04	10	004717.9	38.93	24.19	4
19	1983	04	19	150654.4	40.27	24.05	5
20	1983	04	22	001039.6	38.93	22.85	19
21	1983	04	25	040226.4	38.99	22.52	2
22	1983	05	03	075848.0	39.37	22.97	6
23	1983	06	04	004519.0	40.02	23.58	6
24	1983	06	13	070102.5	39.07	24.16	11
25	1983	06	21	183610.5	38.82	22.35	11
26	1983	07	10	125514.1	39.47	24.26	4
27	1983	08	08	144256.7	39.82	24.28	8
28	1983	08	22	060346.7	39.98	24.22	19
29	1983	10	11	222735.0	39.76	24.08	1
30	1984	01	15	162549.4	39.51	23.48	10
31	1984	05	10	123729.4	40.32	22.76	16
32	1984	05	14	181803.5	40.39	22.87	14
33	1984	06	02	224904.2	41.20	23.19	10
34	1984	07	03	082304.1	41.03	22.54	10
35	1984	07	16	135245.4	39.99	23.71	10
36	1984	10	05	142247.7	40.93	23.48	7
37	1984	10	24	081910.5	39.63	23.29	5
38	1984	12	15	090120.2	39.84	22.76	8
39	1984	12	18	130544.9	39.82	22.85	2
40	1984	12	22	140131.8	39.85	22.87	1
41	1985	02	01	130440.2	40.14	23.20	6
42	1985	03	16	114146.0	41.04	23.98	10
43	1985	03	20	131036.0	40.86	23.59	1
44	1985	05	10	210720.6	40.25	23.28	5
45	1985	06	21	053042.4	40.58	24.20	18
46	1985	07	30	185316.1	40.39	22.79	10



.Scale 1:2500000

FIG. 3 The earthquakes (open polygons: 0Km < depth < 15Km, open squares: 15 Km < depth < 30 Km) and stations (solid triangles) used in this study. The two block configurations are also shown.

coordinates of hypocenter, 50 sec/Km is assigned. To the square root of damping factor of origin time the assigned value is 50 and to that of velocity is 20 sec. The problem was solved with different values of damping factors and only the computed value of the velocities in each block fluctuates. Qualitatively, the results are the same. Therefore, the selected values of damping factors do not affect the results.

As initial values of velocities, 6.0 Km/sec and 6.75 Km/sec are assigned to the upper and lower layer respectively, according to the velocity model used for the determination of hypocenters in the area of Greece.

Then, ray paths from each event to station and travel time through each block are calculated. First, a station and a hypocenter are connected by a straight line. Blocks which the line passes through are found, and the velocities in the blocks are calculated. Fig. 4 shows ray paths from events to stations, which penetrate each block. In the upper layer ray coverage is very good (Fig. 4a). In the lower layer (Fig. 4b) the coverage is rather poor, due to the lack of deeper events.

Because of the high values assigned to the damping factors of events parameters, the data are inverted only one time.

Resolution and covariance (standard error) matrices for path parameters, are also computed.

After that, the whole block configuration is shifted by half block size (15 Km) to the SW direction, as it is shown in Fig. 3.

52 and 30 blocks in the upper and in the lower layer respectively, are penetrated by seismic rays, therefore the effective number of unknown parameters is 266. The inversion procedure is repeated, in order to obtain slight variations of the velocity in the horizontal direction.

Again, resolution and covariance matrices for path parameters are computed.

ΑΠΟΤΕΛΕΣΜΑΤΑ - RESULTS

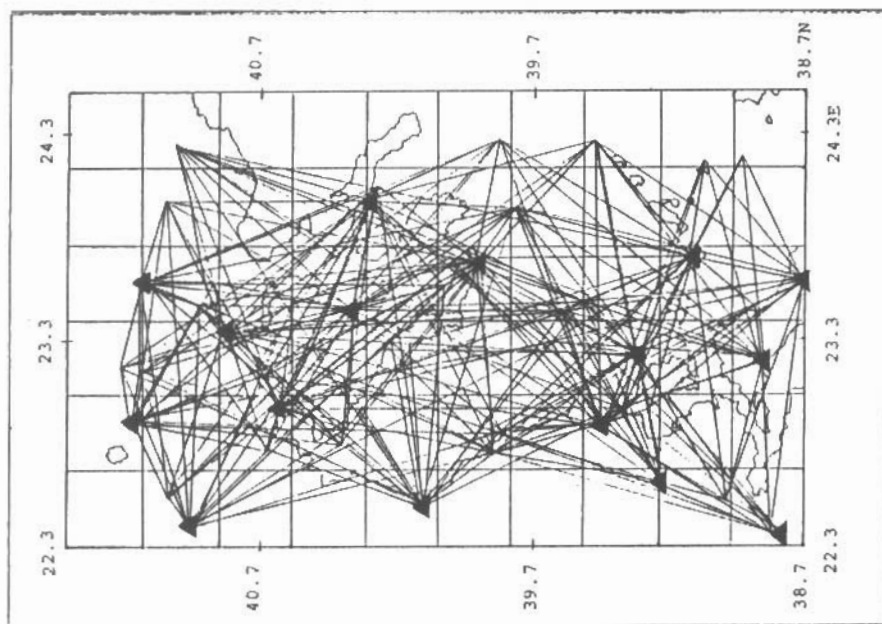
A large number of unknown parameters causes nonunique and unstable solution, but the main good measure of the uniqueness of the i^{th} component of the solution parameters, is the i^{th} diagonal element of resolution matrix.

In Fig. 5 resolution matrices for both layers, for the first and the second block configurations, are shown.

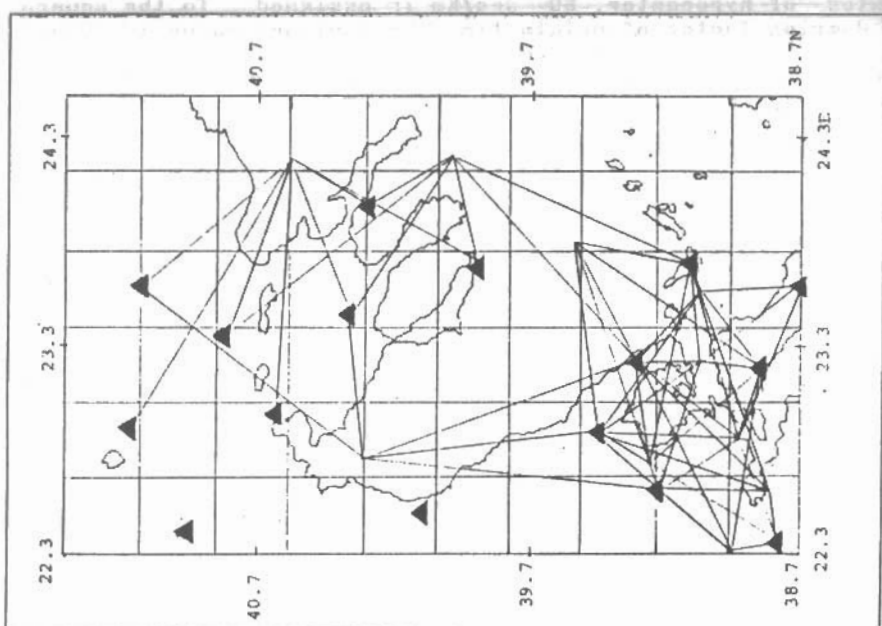
Considering as reliable solutions, those with the diagonal elements of resolution matrix higher than 0.46, it's possible to estimate that the resolution for the upper layer is very good. From the 55 and 52 sampled blocks (for the first and second block configurations) only in 13 blocks (for each configuration) the solution is not resolved well and the values of diagonal elements are less than 0.46.

In the lower layer from the 32 and 30 sampled blocks, for the first and the second block configurations respectively, only in 3 and 7 of them the solution is not resolved well. But generally, the resolution matrix is rather poor and the values of all diagonal elements are around 0.5. For both layers the values of the off-diagonal elements of resolution matrix, are much smaller than those of diagonal elements.

The solution is given as slowness perturbation, in $10^{-2}(\text{Km/sec})^{-1}$, for the first (Fig. 6a) and the second (Fig. 6b) block configurations. Therefore, negatives values correspond to



(a) RAY PATHS Scale 1:2500000



(b) RAY PATHS Scale 1:2500000

Fig. 4. Ray paths used in this study. Solid triangles represent stations. (a): rays which penetrate the top layer. from events occurred in this layer. (b): rays from events occurred in lower layer.

UPPER LAYER

0.60	0.55	0.74	-0.50	0.59	0.01
0.49	0.72	-0.53	0.82	0.54	0.52
0.51	0.72	-0.14	-0.23	0.51	
0.52	0.47	0.34	0.17	0.63	0.52
0.67	0.55	0.67	0.57	0.68	-0.01
0.14	0.58	0.61	0.55	0.48	
0.52	0.64	0.18	0.66	0.55	-0.08
0.52	0.53	0.56	0.31	0.60	0.47
0.51	0.50	0.52	0.55	0.44	0.50

UPPER LAYER

0.53	0.60	0.70	0.02	0.51	0.50	0.49
0.71	0.13	-0.03	0.57	0.51	0.57	0.51
0.74	0.27	-0.20	0.60	0.52	0.60	0.52
0.50	0.36	0.62	0.62	0.53	0.62	0.53
0.68	0.54	0.64	0.51	0.50	0.50	0.50
0.66	0.31	-0.01	0.55	0.00	0.55	0.00
0.56	0.09	0.70	0.58	0.48	0.58	0.48
0.48	0.61	0.52	-0.17	0.52	-0.15	0.48
0.51	0.00	0.49	0.52	0.50	0.50	0.50

LOWER LAYER

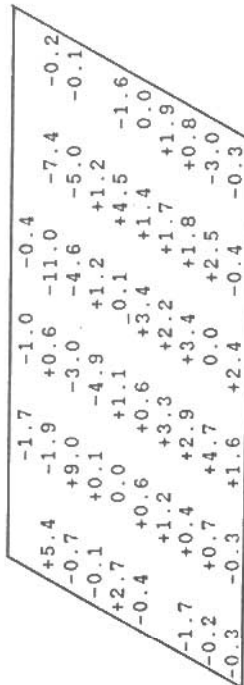
0.50	0.48				
0.44	0.50	0.50	0.48		
0.49	0.52	0.50	0.49		
	0.50	0.50	0.50		
0.47		0.44	0.50		
0.50					
0.50	0.48	0.44	0.50	0.50	
0.48	0.49	0.50	0.50		
0.49	0.50	0.51	0.50		
0.48	0.49	-0.50			

LOWER LAYER

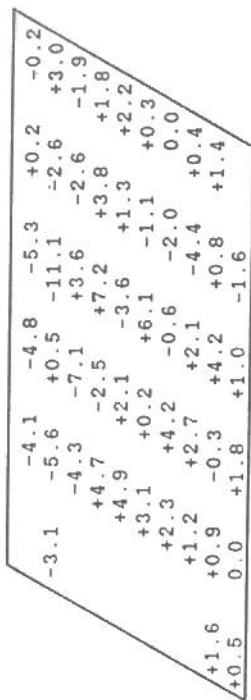
0.49	0.48				
0.50	0.50	0.48	0.44		
	0.50	0.50	0.48		
0.50	-0.50				
0.09	0.52				
0.00	0.48				
0.00		0.45	0.51	0.51	
0.49	0.45	0.50	0.50	0.50	
0.47	0.49	0.50	0.50	0.51	
	0.46			0.49	

Fig. 5 Diagonal elements of resolution matrix for path parameters, in each block of both layers, for the first (a) and second (b) block configurations.

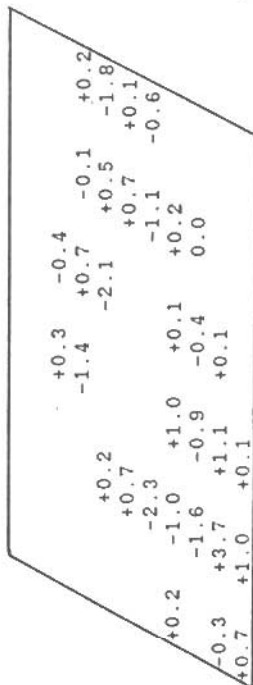
UPPER LAYER



UPPER LAYER



LOWER LAYER



LOWER LAYER

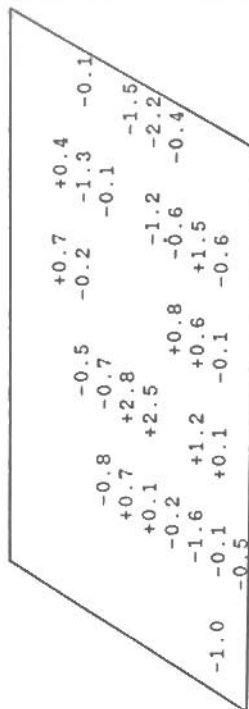


Fig. 6 The solution of inversion shown as slowness perturbation for both layers, in each block, for the first (a) and second (b) block configurations. The unit is 10-2 sec/Km. Negatives and positives values correspond to higher and lower velocities (from the initial values) respectively.

UPPER LAYER

0.36	0.60	0.37	-4.70	0.67	0.00
0.37	0.40	-5.20	0.67	0.58	0.45
0.42	0.46	-3.90	-2.80	0.47	
0.44	0.40	0.28	-0.27	0.74	0.45
0.58	0.44	0.47	0.49	0.65	0.00
	0.27	0.45	0.46	0.38	0.36
0.40	0.43	-0.70	0.42	0.39	0.00
0.39	0.40	0.39	0.40	0.41	0.36
0.37	0.38	0.39	0.38	0.33	0.38

LOWER LAYER

				0.38	0.36
				0.33	0.38
				0.37	0.44
				0.38	0.37
				0.36	0.38
				0.35	0.38
				0.38	0.38
				0.38	0.33
				0.37	0.39
				0.33	0.38
				0.38	0.38
				0.37	0.38
				0.39	0.38
				0.38	0.38
				0.37	0.00
				0.39	0.00
				0.38	0.00

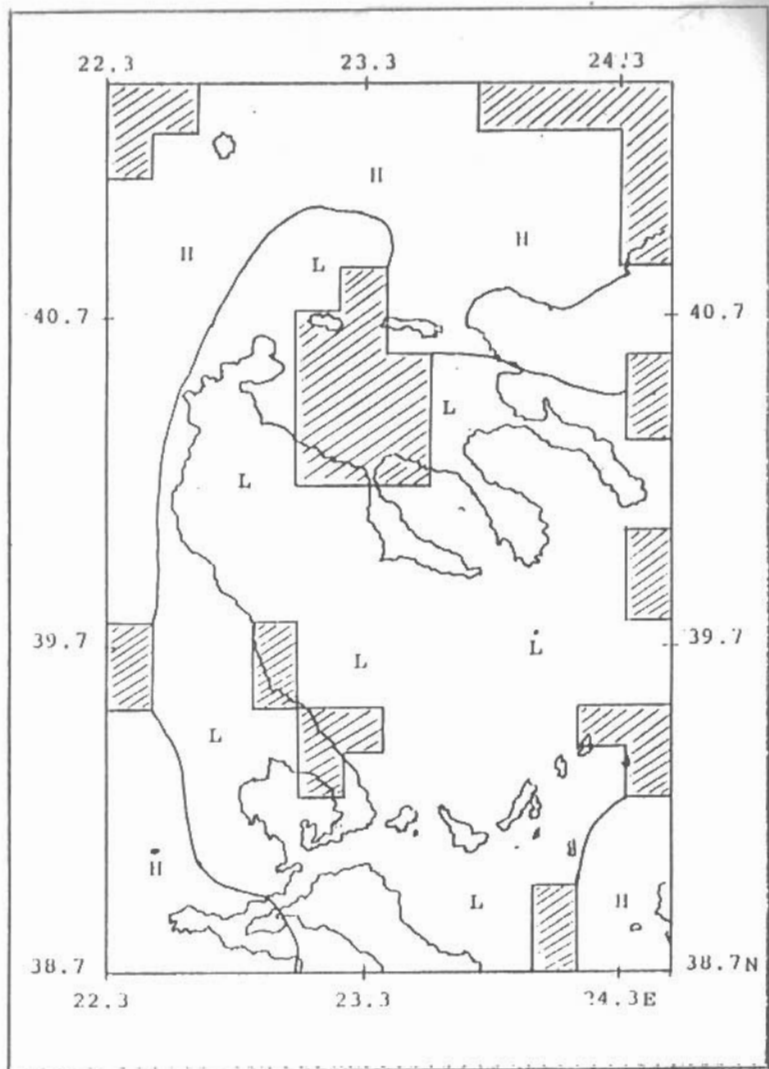
UPPER LAYER

0.42	0.52	0.58	-9.40	0.39	0.36
0.36	-1.20	-1.40	0.50	0.45	
0.43	-0.20	-2.80	0.56	0.44	
0.40	0.29	0.47	0.51	0.43	
0.56	0.44	0.53	0.45	0.41	
0.58	-0.20	-1.45	0.49	0.00	
0.56	0.12	0.66	0.55	0.41	
0.60	0.43	-2.10	0.46	0.02	
0.00	0.41	0.45	0.42		
0.39					
0.44					

LOWER LAYER

					0.34	0.36
					0.41	0.39
					0.39	0.37
					0.41	0.41
					0.41	0.48
					0.00	0.48
					0.00	0.39
					0.00	0.38
					0.40	0.41
					0.36	0.41
					0.41	0.43
					0.41	0.41
					0.42	0.42
					0.42	0.41
					0.38	0.42
					0.42	0.41
					0.40	0.41
					0.41	0.41
					0.41	0.41
					0.39	0.38

Fig. 7 Covariance matrices (standard errors) of the solution, for the velocity structure in both layers of the first (a) and second (b) block configurations are shown. The unit is 10-2 sec/Km.



Scale 1:2500000

Fig. 8 Velocity structure determined by the inversion is shown. The results of two block configurations are superposed, for the upper layer and only for blocks where the magnitude of the diagonal element of resolution matrix is greater than 0.46.

higher (than the initial assigned value) velocity and positive values to lower velocity.

The standard errors, as shown in Fig.7 for both block configurations, are less than $0.67 \times 10^{-2} (\text{Km/sec})^{-1}$, for all blocks and generally are smaller than the estimated slowness perturbation.

The final results of the inversion are shown in Fig. 8 (only for the first layer) after superposition of the solutions of the two block configurations and only for blocks where the magnitude of diagonal element of resolution matrix is greater than 0.46.

Considering that the second layer (between 15 Km and 30Km) is not resolved well and that beneath it there are layers of unknown velocities, it's solution is not included in the final results.

EYZITHEH KAI EYMHEPAEMATA - DISCUSSION AND CONCLUSIONS

Three dimensional velocity structure beneath the crust of Central Greece and the surrounding area is estimated by inversion of P waves arrival times. Due to the lack of deep events only velocity structure of upper crust (15 Km) is estimated.

A careful examination of the results shows the existence of lateral heterogeneities at shallow depth, probably related to the surficial geology.

In the south and central part of the investigated region, low velocities are predominant. These zones correspond very well to the geothermal area and the fracture zones around Pagassitikos Gulf and North Euboea in the South part of the region and to the Sporades graben and sedimentary layers of Thermaikos Gulf in the central part of the region.

In the Northern part of the investigated region there is a high velocity zone well corresponding to the old and stable zones of Rhodope and Servomacedonian massives.

A direct comparison to other relevant studies in the same region is not possible, because the size of sampled blocks in the vertical direction is at least 35 Km (Christodoulou and Hatzfeld, 1987) therefore, the velocity is not affected only by the surficial geology like in the present paper.

BIBΛIOΓPAΦIA - REFERENCES

- Aki, K., W.H.Lee, 1976. Determination of three-dimensional velocity anomalies under a seismic array using first P arrival times from local earthquakes. I A homogeneous initial model. *J. Geophys. Res.*, 81(23), 4381-4399.
- Aki, K., A.Christoffersson and E.S.Husebye, 1977. Determination of the three dimensional seismic structure of the lithosphere. *J. Geophys. Res.*, 82, No 2, 277-296.
- Christodoulou, A. and Hatzfeld, D., 1987. Inversion of the crustal and upper mantle structure beneath Chalkidiki (Northern Greece). Submitted for publication.
- Comninakis, P.E. and B. C. Papazachos, 1981. Properties of the main seismic zone in Northern Greece and surrounding area. *Proc. Conf. Intracontinental Earthquakes, Ohrid, Yugoslavia*, 173-186.
- Dewey, J.F., and Sengör, A.M.C., 1979. Aegean and surrounding region: complex multiplate and continuum tectonics in a convergent zone. *Bull. Geol. Soc. Am.*, 90, 84-92.
- Drakopoulos, J. and Delibasis N., 1982. The focal mechanism of

- earthquakes in the major area of Greece the period 1947-1981. Univ. of Athens, Seism. Lab., Publ. No 2, 1-72.
- Faugères, L. and Robert, C., 1976. Etudes Sédimentologique et Minéralogique de deux forages sur le Golf Thermaïque (Mer Egée). Ann. Univ. Provence, Géol. Méditer., III, 4, 209-218.
- Fytikas, M., Giuliani, O., Innocenti, F., Marinelli, G. and Mazzuoli, R., 1976. Geochronological data on recent magmatism of the Aegean Sea. Tectonophysics, 31, T29-T34.
- Hashida, T., Stavrakakis, G. and Shimazaki, K., 1987. Three-dimensional seismic attenuation structure beneath the Aegean region and its tectonic implication. In press, Tectonophysics.
- Horie, A. and Aki, K., 1982. Three-dimensional velocity structure beneath the Kanto District, Japan. J. Phys. Earth, 30, 255-281.
- Ishida, M., 1984. The spatial distribution of earthquake hypocenter and the three-dimensional velocity structure in the Kanto Tokai District, Japan. J. Phys. Earth, 32, 399-422.
- Levenberg, K., 1944. A method for the solution of certain non linear problems in least squares. Quart. Appl. Math., 2, 164-168.
- Makris, J., 1975. Crustal structure of the Aegean Sea and Hellenides obtained from geophysical surveys. J. Geophys. Res., 41, 441-443.
- Makris, J., 1978(a). Some geophysical considerations on the geodynamic situation in Greece. Tectonophysics, 46, 251-268.
- Makris, J., 1978(b). The crust and upper mantle of the Aegean region from deep seismic soundings. Tectonophysics, 46, 269-284.
- McKenzie, D., 1972. Active tectonics of the Mediterranean region. Geophys. J. R. Astr. Soc., 30, 109-185.
- McKenzie, D., 1978. Active tectonics of the Alpine-Himalayan belt: the Aegean Sea and surrounding regions. Geophys. J. R. Astr. Soc., 55, 217-254.
- Ninkovitch, D. and Hays, J. D., 1972. Mediterranean island arcs and origin of high potash volcanoes. Earth and Planet. Sc. Lett., 16, 331-345.
- Papazachos, B. C. and Comninakis, P. E., 1978. Deep structure and tectonics of the Eastern Mediterranean. Tectonophysics, 46, 285-296.
- Papazachos, B. C., Moundrakis, D., Psilovikos, A. and Leventakis, G., 1979(a). Surface fault traces and fault plane solutions of the May-June 1978 major shocks in Thessaloniki area, Greece. Tectonophysics, 53, 171-183.
- Pavlis, G. L., and J. R. Booker, 1980. The mixed discrete-continuous inverse problem: Application to the simultaneous determination of earthquake hypocenters and velocity structure. J. Geophys. Res., 85, 4801-4810.
- Spakman, W., 1986. Subduction beneath Eurasian in connection with the Mesozoic Tethys. In press, Geol. Mijnbouw.
- Spencer, C. and D. Gubbins, 1980. Travel-time inversion for simultaneous earthquake location and velocity structure determination in laterally varying media. Geophys. J. R. Astron. Soc., 63, 95-116.
- Wiggins, R. A., 1972. The general linear inverse problem: Implications of surface waves and free oscillations for earth structure. Geophys. Space Phys., 10, 251-285.